Optical referencing technique with CW lasers as intermediate oscillators for continuous full delay range frequency comb interferometry

Jean-Daniel Deschênes,[1] **Philippe Giaccari,**[2] **and Jérôme Genest**[1,*]

[1]*Centre d'optique, photonique et laser, 2375 rue de la Terrasse, Université Laval, Québec, Québec, Canada, G1V 0A6, Canada*
[2]*Now with ABB Switzerland, Segelhof 9P, 5405 Baden-Dättwil, Switzerland*
**jgenest@gel.ulaval.ca*

Abstract: This paper presents a significant advancement in the referencing technique applied to frequency comb spectrometry (cFTS) that we proposed and demonstrated recently. Based on intermediate laser oscillators, it becomes possible to access the full delay range set by the repetition rate of the frequency combs, overcoming the principal limitation observed in the method based on passive optical filters. With this new referencing technique, the maximum spectral resolution given by each comb tooth is achievable and continuous scanning will improve complex reflectometry measurements. We present a demonstration of such a high resolution cFTS system, providing a spectrometry measurement at 100 MHz of resolution (0.003 cm^{-1}) with a spectral signal to noise ratio of 440 for a 2 seconds measurement time. The resulting spectrum is composed of $105 \cdot 10^3$ resolved spectral elements, each corresponding to a single pair of optical modes (one for each combs). To our knowledge, this represents the first cFTS measurement over the full spectral range of the sources in a single shot with resolved individual modes at full resolution.

OCIS codes: (120.3940) Metrology; (120.4640) Optical instruments; (140.4050) Mode-locked lasers; (300.6300) Spectroscopy, Fourier transforms.

References and links

1. F. Keilmann, C. Gohle, and R. Holzwarth, "Time-domain mid-infrared frequency-comb spectrometer," Opt. Lett. **29**, 1542–1544 (2004).
2. I. Coddington, W. C. Swann, and N. R. Newbury, "Coherent Multiheterodyne Spectroscopy Using Stabilized Optical Frequency Combs," Phys. Rev. Lett. **100**, 013902 (2008).
3. P. Giaccari, J.-D. Deschênes, P. Saucier, J. Genest, and P. Tremblay, "Active Fourier-transform spectroscopy combining the direct RF beating of two fiber-based mode-locked lasers with a novel referencing method," Opt. Express **16**, 4347–4365 (2008).
4. T. Yasui, Y. Kabetani, E. Saneyoshi, S. Yokoyama, and T. Araki, "Terahertz frequency comb by multifrequency-heterodyning photoconductive detection for high-accuracy, high-resolution terahertz spectroscopy," Appl. Phys. Lett. **88**, 241104 (2006).
5. A. Bartels, A. Thoma, C. Janke, T. Dekorsky, A. Dreyhaupt, S. Winnerl, and M. Helm, "High-resolution THz spectrometer with kHz scan rates," Opt. Express **14**, 430–437 (2006).
6. S. Kray, F. Spöler, M. Först, and H. Kurz, "Dual femtosecond laser multiheterodyne optical coherence tomography," Opt. Lett. **33**, 2092–2094 (2008).

#134906 - $15.00 USD Received 9 Sep 2010; revised 15 Oct 2010; accepted 15 Oct 2010; published 20 Oct 2010

7. I. Coddington, W. C. Swann, and N. R. Newbury, "Coherent linear optical sampling at 15 bits of resolution," Opt. Lett. **34**, 2153–2155 (2009).
8. G. Taurand, P. Giaccari, J.-D. Deschênes, and J. Genest, "Time Domain Optical Reflectometry Measurements Using a Frequency Comb Interferometer," Appl. Opt. **49**, 4413–4419 (2010).
9. B. Bernhardt, A. Ozawa, P. Jacquet, M. Jacquey, Y. Kobayashi, T. Udem, R Holzwarth, G. Guelachvili, T. W. Hansch, and N. PicquÈ, "Cavity-enhanced dual-comb spectroscopy," Nat. Photonics **4**, 55–57 (2009).
10. N. R. Newbury and W. C. Swann, "Low-noise fiber-laser frequency combs (Invited)," J. Opt. Soc. Am. B **24**, 1756–1770 (2007).
11. C. Dorrer, D. C. Kilper, H. R. Stuart, G. Raybon, and M. G. Raymer, "Linear Optical Sampling," IEEE Photon. Technol. Lett. **15**, 1746–1748 (2003).
12. J. Reichert, R. Holzwarth, Th. Udem, and T. W. Hansch, "Measuring the frequency of light with mode-locked lasers," Opt. Commun. **172**, 59–68 (1999).
13. C. Turcotte, "Laser a semi-conducteurs utilise comme reference metrologique dans un spectrometre par transformee de Fourier: effet du bruit," Master's thesis, Universite Laval, (1999).
14. N. R. Newbury, I. Coddington, and W. C. Swann, "Sensitivity of coherent dual-comb spectroscopy," Opt. Express **18**, 7929–7945 (2010).
15. W. C. Swann, J. J. McFerran, I. Coddington, N. R. Newbury, I. Hartl, M. E. Fermann, P. S. Westbrook, J. W. Nicholson, K. S. Feder, C. Langrock, and M. M. Fejer, "Fiber-laser frequency combs with subhertz relative linewidths," Opt. Lett. **31**, 3046–3048 (2006).

1. Introduction

The technique of using two pulsed sources with detuned repetition rates to generate a sliding delay between the pulses has already been proven to produce quality interferograms (IGM), enough to accomplish active spectroscopy [1–5] and measure impulse responses [6–8]. The most challenging aspect of producing usable cFTS measurements is to generate two pulse trains with a linearly increasing delay between each pulse pair with enough precision over the complete measurement time. The timing and phase between the two pulses must be accurate to within a fraction of an optical cycle (5 fs at 1550 nm). In the papers from the NIST group [2,7], the repetition rates and the carrier-to-enveloppe offset (CEO) frequencies are stabilized using an elaborate setup with two CW lasers with Hz-level linewidth. In other demonstrations [1,9], each interferogram is acquired over a very short time and significant differences are reported between successive interferograms, preventing averaging to improve the signal to noise ratio (SNR). An alternative approach to circumvent these problems is to use a referencing technique such as the method proposed in [3] to track the fluctuations in the parameters of the sources, and to properly account for these differences in post-processing. The referencing technique was previously limited in the optical delay that could be corrected and thus in spectral resolution achievable. This limitation was a consequence of using optical filters with an impulse response that would decay after around 500 ps, corresponding to an equivalent optical path difference (OPD) of 10 cm in a Michelson Interferometer. The improved version described here uses continuous-wave (CW) lasers as intermediate oscillators to generate the same information over the complete delay range, thus allowing to use the complete spectral resolution set by the repetition rates of the lasers. In our case, with repetition rates of 100 MHz, the equivalent OPD is around 3 m. It is important to note here that the referencing lasers are not used to stailize the frequency comb sources but only to provide the RF signature required for the referencing post-treatment.

To succesfully perform interferometric measurements using two combs, the difference in the pulse train period, ΔT_r must be constant for every pulse pair. If this parameter drifts over the course of a measurement, the effect will be the same as a speed change of a moving mirror in a conventional Michelson interformeter: the delay axis of the measurement will be distorted. If this interferometer is used to produce spectroscopic measurements, this introduces smearing of the spectral features and/or noise. Two approaches are possible to eliminate this problem: one can monitor the parameter and actively adjust the frequency comb sources using feedback

#134906 - $15.00 USD Received 9 Sep 2010; revised 15 Oct 2010; accepted 15 Oct 2010; published 20 Oct 2010

loops [10], or the parameters fluctuations can simply be continuously monitored and taken into account during the post-treatment process. The results presented in this paper are based on the second approach.

The problem of measuring the delay between a single pulse pair is most easily solved by filtering the pulses with a narrow-band filter; this will give an interference signal which is function of the center frequency of the optical filter and the delay. Thus, knowing the center frequency, one can recover the delay axis from the recorded signal. However, in a comb Fourier Transform Spectrometer (cFTS), there are two parameters required to describe the interference signal. In addition to the time difference between each pulse in a pair, each pair can potentially have a different phase difference relative to their envelope. In fact, in the pulse train output from a perfectly stabilized frequency comb, the phase of each pulse slides linearly at a fixed rate with respect to the envelope. In practice however, even with state-of-the-art stabilization, there still remains some jitter of this carrier-to-envelope phase offset (CEO) [10]. This justifies the need to also track this parameter. When both parameters are measured, it turns out that performing tight stabilization is no longer necessary for most practical applications, such as spectrometry and reflectometry. In that situation, it was already demonstrated that the source instabilities can be corrected mathematically during post-processing.

The paper is organized in the following way: section 2 provides a condensed version of the post-treatment algorithm already presented in [3] and adapted to the new active referencing system; section 3 describes the new active referencing technique; section 4 presents the spectrometry experimental results; section 5 exposes a technique for SNR improvement by pulse chirping and section 6 discusses the similarities between the referencing algorithm and stabilization of the frequency combs on the CW lasers. Finally, appendix A presents the mathematical derivations for the referencing signals.

2. Post-correction algorithm

To be able to correctly track the repetition rate and CEO difference between the two lasers, two reference signals at two optical frequencies have to be monitored. Both signals can be produced by narrow bandpass filters, each at a different frequency. Following the derivation in appendix A, the referencing signals are:

$$r_{1d}[k] = A_1(\Delta T_r(k)) \exp\left[j2\pi f_{c1}\Delta T_r(k) + j\Delta\varphi(k)\right], \tag{1}$$

$$r_{2d}[k] = A_2(\Delta T_r(k)) \exp\left[j2\pi f_{c2}\Delta T_r(k) + j\Delta\varphi(k)\right], \tag{2}$$

where k is the index of the pulse pair, $\Delta T_{r1}(k)$ is the difference in pulse arrival time for each pulse pair, $\Delta\varphi(k)$ is the difference in pulse phase for each pulse pair, A_1 and A_2 are the slowly varying part of the bandpass filters impulse response, f_{c1} and f_{c2} are the center frequencies of the bandpass filters.

The interference of both pulse trains, when one of the pulse train is filtered by an arbitrary sample, produces an electrical signal:

$$s_{md}[k] = A_m(\Delta T_r(k)) \exp\left[j2\pi f_m\Delta T_r(k) + j\Delta\varphi(k)\right], \tag{3}$$

with $A_m(\tau)$ being the slowly varying part of the sample's impulse response filtered by the probing pulse's shape and the time-reversed shape of the other pulse shape (see appendix A). $A_m(\tau)$ is the quantity of interest and contains all the information on the sample's linear response to any input within the bandwidth of the pulses. Removing the effect of the pulses on the measurement can be made by deconvolution with the shape found by with a calibration procedure, e.g. by measuring the inteferogram produced by the system without any sample. In the experimental demonstration presented in this paper, the sample is a gas cell with very narrow absorption

#134906 - $15.00 USD Received 9 Sep 2010; revised 15 Oct 2010; accepted 15 Oct 2010; published 20 Oct 2010

lines and the shape of the pulse's spectrum varies much more slowly than the interesting features; such a removal was not deemed necessary to demonstrate the validity of the correction algorithm.

The first step of the correction algorithm is to cancel fluctuations from $\Delta\varphi(k)$:

$$s_{md}[k]\frac{r_{1d}^{*}[k]}{\|r_{1d}[k]\|} = A_m(\Delta T_r(k))\exp\left[j2\pi(f_m - f_{c1})\Delta T_r(k)\right]. \tag{4}$$

This assumes that $A_1(\tau)$ is real, ie $\angle(A_1(\tau)) = 0$. This is a constraint on the optical filters used. There must be no chirp in the impulse response. In practice, this constraint is met with uniform Fiber Bragg Gratings (FBG) which were used in the first referencing implementation [3].

This first algorithmic step removes all dependence on $\Delta\varphi(k)$. Note that this first step removes all fluctuations measured at f_{c1}; both the CEO and repetition rate fluctuations for this frequency are cancelled. Also, $f_m - f_{c1}$ is much smaller than f_m, in a ratio of about $1:200$ in our system. The sensitivity of the carrier $exp[...]$ to jitter in $\Delta T_r(k)$ is thus accordingly reduced. The last step of the algorithm is to resample the signal on a new temporal grid such that $\Delta T_r(k)$ has constant increments from sample to sample. This grid is easily computed from the phase of the signal:

$$r_{grid}[k] = \frac{r_{1d}^{*}[k]r_{2d}[k]}{\|r_{1d}[k]\|\|r_{2d}[k]\|} = \exp\left[j2\pi(f_{c2} - f_{c1})\Delta T_r(k)\right]. \tag{5}$$

It should be noted that when extracting the phase from the signal described in Eq. (5), a large span between the two chosen frequencies f_{c2} and f_{c1} is desirable, since this reduces the sensitivity to additive noise. The actual implementation of the algorithm differs from this description only from the fact that digital filters need to be used to generate the complex representation of the signals as well as removing some noise.

3. New implementation

The referencing scheme using narrow bandpass filters like FBGs has two main disadvantages: (1) only a small portion of the delay range produces usable reference signals and (2) the remaining signal is weak. Using filters with longer impulse reponses would imply having even less power (they would have less bandwidth). To circumvent both these problems, we propose to use two CW lasers as intermediate oscillators and to digitally compute the beating of the resulting signals. This way, the phase fluctuations of the CW laser will be subtracted, yielding the beating of only one mode for each frequency comb.

To accomplish this, four signals are measured. Each signal is the linear optical sampling [11] of one CW laser by one of the frequency combs. Optical bandpass filters are used to filter the frequency combs around the wavelength of the CW lasers to reduce the shot noise contribution and thus to improve the SNR [12]. Figure 1 depicts the complete measurement setup, where the branches that are connected to analog-to-digital converters (ADCs) 1 to 4 provide the reference signals. The signals at the output of the photodetectors are electrically sampled to yield:

$$s_{1d}[k] = \sqrt{P_{CW1}P_{FC1,\lambda 1}}\exp\left[j2\pi f_{cw1}T_{r1}(k) + j\varphi_1(k) + j\varphi_{CW1}(kT_{r1})\right], \tag{6}$$

$$s_{2d}[k] = \sqrt{P_{CW1}P_{FC2,\lambda 1}}\exp\left[j2\pi f_{cw1}T_{r2}(k) + j\varphi_2(k) + j\varphi_{CW1}(kT_{r2})\right], \tag{7}$$

$$s_{3d}[k] = \sqrt{P_{CW2}P_{FC1,\lambda 2}}\exp\left[j2\pi f_{cw2}T_{r1}(k) + j\varphi_1(k) + j\varphi_{CW2}(kT_{r1})\right], \tag{8}$$

$$s_{4d}[k] = \sqrt{P_{CW2}P_{FC2,\lambda 2}}\exp\left[j2\pi f_{cw2}T_{r2}(k) + j\varphi_2(k) + j\varphi_{CW2}(kT_{r2})\right], \tag{9}$$

where k is the index of the digital sample, P_{CWx}, f_{cwx} and ϕ_{CWx} are respectively the power, the frequency and the phase deviation of each CW laser. P_{FCx,λ_y} is the power of the frequency comb

#134906 - $15.00 USD Received 9 Sep 2010; revised 15 Oct 2010; accepted 15 Oct 2010; published 20 Oct 2010

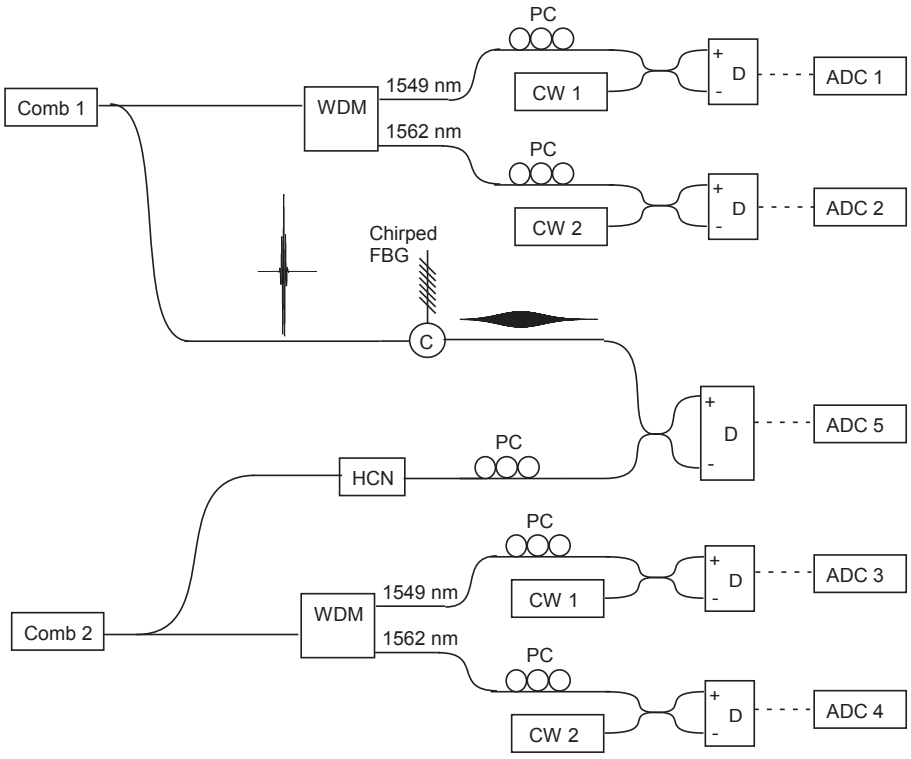

Fig. 1. Experimental setup. Solid lines = optical fiber, dashed lines = electrical cable, WDM = Wavelength division multiplexer, PC = Polarization controller, FBG = Fiber Bragg Grating, D = Balanced detector, ADC = Analog to digital converter.

x around wavelength λ_y. These signals are digitally combined to produce the two referencing signals:

$$r_{1d}[k] = s_{1d}[k]s^*_{2d}[k], \tag{10}$$
$$r_{2d}[k] = s_{3d}[k]s^*_{4d}[k]. \tag{11}$$

Expanding, we get:

$$\begin{aligned} r_{1d}[k] &= P_{CW1}\sqrt{P_{FC1,\lambda 1}P_{FC2,\lambda 1}}\times \\ &\quad \exp\left[j2\pi f_{cw1}\Delta T_r(k) + j\Delta\varphi(k) + j\varphi_{CW1}(T_{r1}(k)) - j\varphi_{CW1}(T_{r2}(k))\right], \end{aligned} \tag{12}$$

$$\begin{aligned} r_{2d}[k] &= P_{CW2}\sqrt{P_{FC2,\lambda 1}P_{FC2,\lambda 1}}\times \\ &\quad \exp\left[j2\pi f_{cw2}\Delta T_r(k) + j\Delta\varphi(k) + j\varphi_{CW2}(T_{r1}(k)) - j\varphi_{CW2}(T_{r2}(k))\right]. \end{aligned} \tag{13}$$

Note that the signals could also be multiplied prior to sampling using analog mixers. The reason to do it digitally is because of the flexibility in choosing the bandpass filters, the linear phase caracteristic of digital filters which is impossible in analog filters and overall ease of use of the setup. The signals given by this new scheme [Eqs. (12) and (13)] are equivalent to those in Eqs. (1) and (2), with only minor differences. The frequencies of the two CW reference lasers now scale the delay axis, playing the role of the central frequencies of the filters. Also,

#134906 - $15.00 USD Received 9 Sep 2010; revised 15 Oct 2010; accepted 15 Oct 2010; published 20 Oct 2010

the phase term $\varphi_{CW1}(kT_{r1}) - \varphi_{CW1}(kT_{r2})$ is not present in the first equations. This term is in fact the difference in the phase of the CW laser between two successive instants. For zero optical delay between the pulses, this term is necessarily zero, while at the largest delay between these two instants, that is the period of the pulse train, T_r, this term is maximal. This sets a constraint on the type of CW laser used in this scheme; the phase difference between the electrical field of the CW laser at time t and at time $t + T_r$ must be small. Relatively cheap narrow-linewidth lasers easily meet this criterion for our value of 10 ns for T_r. We use PLANEX lasers from Redfern Integrated Optics which have 30 kHz of linewidth. Assuming white frequency noise, this implies a standard deviation of $\sqrt{2\pi\nu T} = 43$ mrad of phase difference at 10 ns of delay. It must be pointed out that this requirement of small phase fluctuation at a certain delay is exactly the same requirement which applies to a reference laser in a Michelson interferometer with the same optical delay between the two arms [13]. The effect of the residual phase is mostly phase noise on the corrected interferogram, with a variance that scales linearly with the optical delay.

The advantage of this technique is that the reference signals now have a constant power, independent on the optical delay between the pulses and thus the full delay range is accessible. Also, the signals have a potentially much larger amplitude due to P_{CW1} providing coherent gain. In the previous referencing scheme, the signal was produced by the interference of two filtered pulse trains, while in the new scheme, the signals are produced by the interference of one high-power CW laser ($\approx$ 10 mW, divided in 4 paths) with each filtered pulse train. The pulse trains after the filters (ITU grid filters with 50 GHz of bandwidth) have 15 μW of power.

4. Results

To prove the validity of this technique, we performed a spectroscopic measurement of hydrogen cyanide (HCN) around 1550 nm. The experimental setup is depicted in Fig. 1. The frequency combs are generated by two Menlo Systems Inc. lasers at 100 MHz repetition rate. The bandwidth of the pulses is approximately 100 nm around 1562 nm (12 THz around 192 THz). The pulse width is approximately 90 fs when dispersion is completely compensated and the average power is 15 mW. The gas is in a calibration cell with fibers having APC connectors. The explanation for including a chirped FBG in the path of one laser is provided in section 5 (basically for SNR improvement). We record the interference signal produced by one comb filtered by the HCN sample with the other unfiltered comb. To measure a transmittance using this setup, one could record the interference signal produced by the unfiltered frequency combs, either in parallel or in a subsequent step. The spectral transmittance could be computed from the ratio of the spectra obtained after correction.

The repetition rate difference between the frequency combs is 100 Hz, stabilized by a slow digital feedback loop (4 Hz update rate) which actuates a piezo stretcher in the cavity. Although an analog phased-locked loop with kHz of bandwidth is available in our setup, it is unecessary and conterproductive to use it as it actually introduces more noise into the system, mainly due to the reference electronic oscillator. Folding is avoided in our measurements by manually tuning the repetition rate and/or CEO frequency of the combs to place the beating in the center of the spectrum. The frequency of the reference beating are placed away from zero frequency and Nyquist frequency (50 MHz) by tuning the pump current to the CW lasers by another slow digital feedback loop.

The repeating interferogram pattern is produced every 10 ms, as the pulses from both frequency combs are coincident temporally on the detector.

The measurement time is 2 sec, limited by the amount of memory of our data acquisition card (GaGe Octopus, 14 bits at 125 MS/s).

After acquisition, the data is corrected using the algorithm described in section 2. Due to the different fiber paths between the reference and measurement paths, slow drifts accumulate over

#134906 - $15.00 USD Received 9 Sep 2010; revised 15 Oct 2010; accepted 15 Oct 2010; published 20 Oct 2010

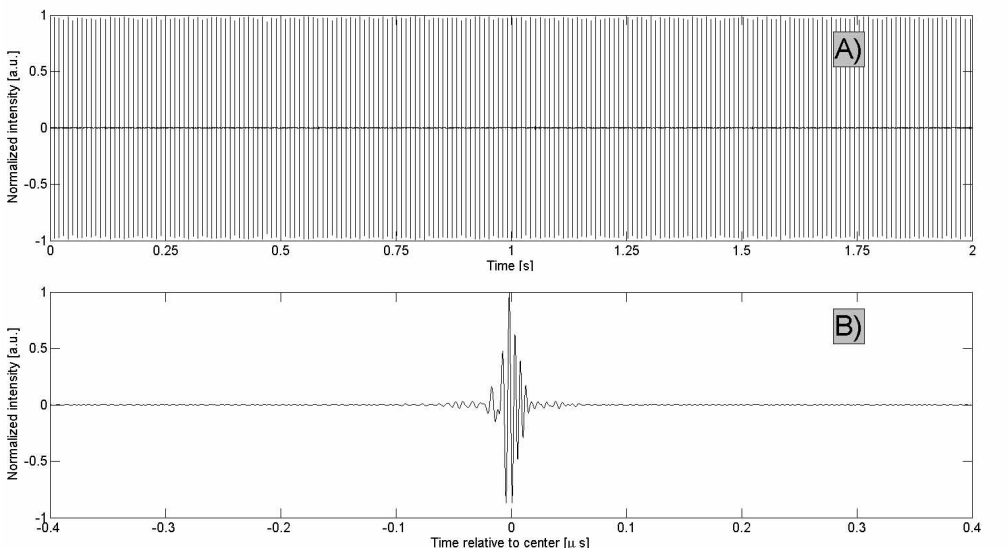

Fig. 2. Corrected IGMs after correction and deconvolution (dispersion compensation). A) Complete measurement set. Each vertical line corresponds to a single IGM. B) Zoom on a single IGM.

time between the reference and measurement paths. These slow drifts are tracked by cross-correlation of each IGM with the first IGM; this gives both the position and phase of each corrected interferogram and the fluctuations in both parameters are removed from the corrected data. The cross-correlation was chosen because it gives the best signal-to-noise ratio of any linear method to estimate the delay and is unbiased. In this particular measurement set, these drifts correspond to at most 16 μm of OPD and 1 rad of phase and are attributed to mechanical vibrations and thermal fluctuations of the fiber paths, as the referencing and measurement setup are placed on separate optical tables, linked by two 10 m cables. The post-correction IGM are presented in Fig. 2.

Performing the Fourier transform on the complete measurement yields as expected a spectrum with discrete modes, as shown in Fig. 3(C). Each mode corresponds to the beating of one pair of optical modes of the frequency combs. Before correction, the mutual coherence time for the beating of one mode of each frequency comb is 10 μs, as computed from one of the reference signals, which yields a linewidth before correction on the order of 100 kHz. The full-width at half-maximum (FWHM) of a sinc lineshape for a measurement time of 2 sec is $1.2/(2\text{ s}) = 0.6$Hz. It is interesting to note that the correction method recovers the full coherence between the interferograms even for such a long measurement time, as seen from the width of 0.6 Hz of the individual modes in Fig. 3(D). Although performing such a long Fourier transform validates that the coherence is recovered by the referencing, in practice it is less computationally intensive to first segment the measurement into individual IGMs and to average them before performing a smaller Fourier transform. As expected, this averaging yields an IGM with an SNR equal to the SNR of a single IGM before averging times the square root of the number of IGMs in the average. The segmentation of the different IGMs is easily done after resampling as the resampled vectors are on an equidistant OPD grid. This produces the same result as evaluating the spectrum only at the discrete modes of the beating, as is shown by the red line on Figs. 3(A)–3(C).

It must be pointed out that the referencing technique does not provide an absolute calibrated

#134906 - $15.00 USD Received 9 Sep 2010; revised 15 Oct 2010; accepted 15 Oct 2010; published 20 Oct 2010

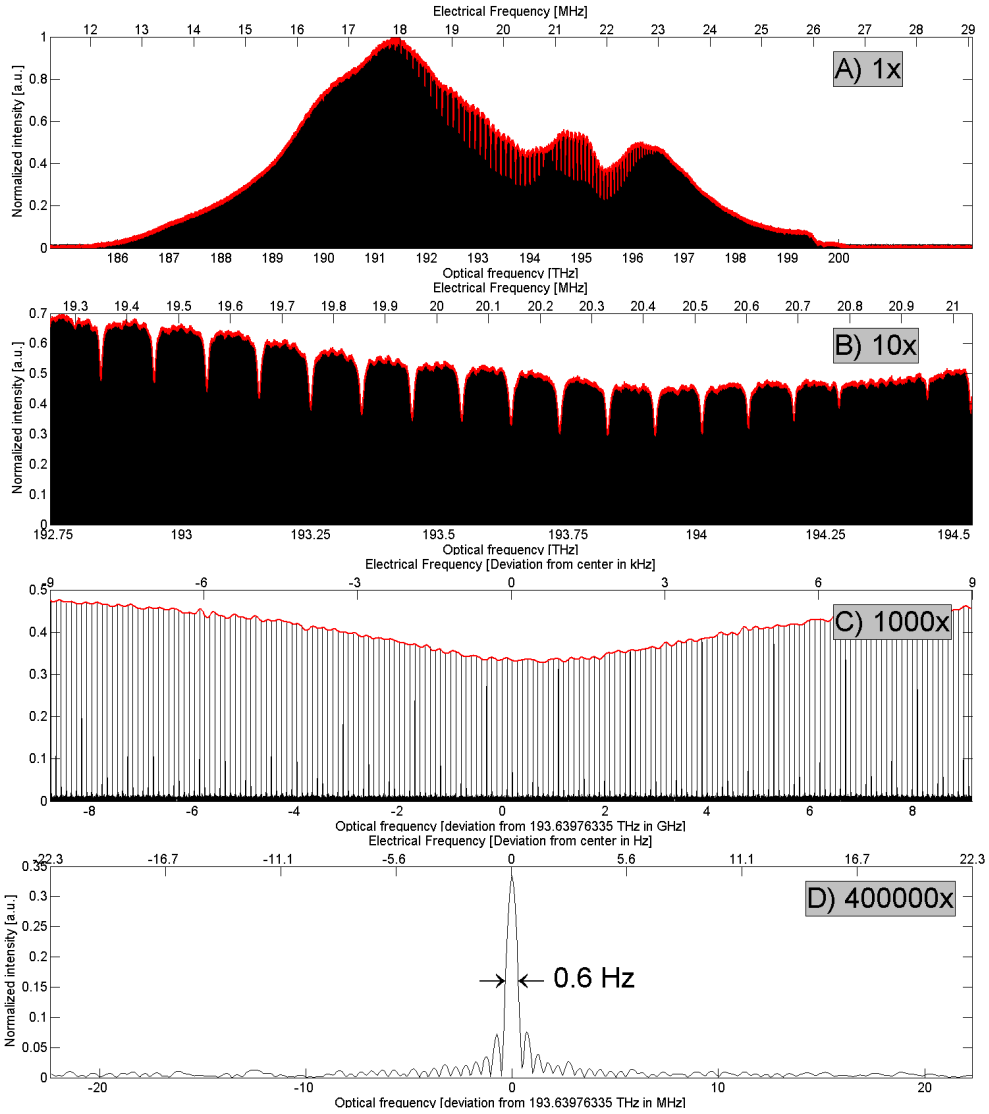

Fig. 3. Spectrum of the complete corrected measurement (black) and spectrum of the average of the segmented IGMs (red). The features seem on (A) and (B) are absorption lines of the sample. In (C), the slow variation is a single absorption line and each vertical line corresponds to a single of beating mode. Part (D) shows a single transform-limited mode.

#134906 - $15.00 USD Received 9 Sep 2010; revised 15 Oct 2010; accepted 15 Oct 2010; published 20 Oct 2010

frequency scale, it only guarantees that it will be linear between the two reference frequencies. The displayed frequency grid in Fig. 3 is thus simply a linear interpolation between the known frequencies of the two reference CW lasers. The accuracy of the computed frequency grid is thus directly linked to the knowledge of the absolute optical frequencies of the reference lasers, which in our case are known to better than $\approx$ 10 GHz. Also, any unaccounted deviation in the frequency of one CW laser from one measurement to another will change the frequency scale such that, strictly speaking, successive interferograms can no longer be co-added without error. In our case, with the PLANEX lasers, the frequency drifts for less than 100 kHz over the course of one measurement and the error this introduces in the OPD axis was estimated to be significantly smaller than the drifts in the paths. Although no attempt to produce a calibrated frequency scale was made in this paper, one could use a known molecular spectrum and infer the frequency grid from the position of the absorption lines, as in done in conventional FTS.

The structure at approximately 10 GHz is thought to come from the transmission spectrum of the chirped FBG used to stretch the IGMs. If a transmittance is computed with respect to a sample-less measurement, it could theoretically be cancelled.

The peak spectral SNR is measured as the ratio of the peak spectrum value to the standard deviation of the out-of-band noise and gives a value of 440 for this 2 seconds measurement. The number of resolved spectral elements is equal to the number of modes in the spectrum. Because of the irregular shape of the spectrum, we use the root-mean squared width as the metric for the number of resolved spectral elements: $M = 1.05 \cdot 10^5$. The actual number of modes is a little higher than this value, but this definition eliminates any ambiguity on which modes are sufficiently higher than the noise to count as one spectral element. The spectral elements are all measured at the same time in a a single measurement. This gives a factor of merit of $M \cdot \mathrm{SNR}/\sqrt{T} = 4 \cdot 10^7$, according to the definition given in [14].

5. Dynamic range reduction for SNR improvement

As explained in [14], cFTS systems are prone to a limitation of sensitivity due to the large dynamic range required. This limitation comes from the fact that the largest detected signal is limited in amplitude by the detector's linear range, and the minimum signal is limited by the detector's thermal noise. In our setup, we circumvent this problem by stretching (in the time delay axis) the pulses of one of the frequency combs by a chirped fiber Bragg grating (this solution is also very interesting to probe samples that could be damaged by high peak power pulses, for example biological samples). This lowers the dynamic range of the resulting interferogram and improves the signal-to-noise ratio. Chirping one of the pulse train spreads the IGM over a larger duration, but preserves it's energy. This way, more power can be sent to the detector to increase the total signal energy without causing saturation of the detector. The drawback of using this technique to reduce the dynamic range is that because the noise induced by timing jitter is spread over a larger OPD range, the equivalent noise in the spectral domain will be less correlated than a similar measurement without stretching. This will accordingly reduce the accuracy of a baseline removal technique. However, when the dominant noise is additive noise, the SNR effectively increases because of stretching until the phase noise becomes the dominant contribution and the additive noise is effectively suppressed. Of course, the amount of additive noise is dependent upon OPD range so the optimum of this trade-off will vary with the desired resolution. More careful studies are required to predict the optimum amount of stretching for a certain desired resolution, depending on the amount of residual jitter and additive noise.

This stretching affects only the phase of the computed spectrum and the magnitude is the same as without stretching and hence no further processing is necessary for spectroscopy measurements. For measurements where the width of the IGM's centerburst determines the resolution, e.g. in reflectometry measurements [8], one can simply characterize the dispersion

#134906 - $15.00 USD Received 9 Sep 2010; revised 15 Oct 2010; accepted 15 Oct 2010; published 20 Oct 2010

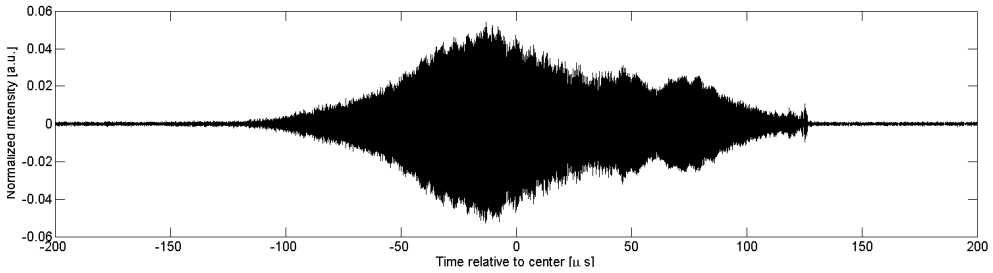

Fig. 4. Chirped IGM. Note the much larger horizontal scale and the 20 times lower peak value compared to the deconvolved IGM of Fig. 2(B).

introduced by this device and remove it by deconvolution. Figure 4 presents a chirped IGM before deconvolution, while the IGM of Fig. 2(B) is taken after the deconvolution step. It must be noted that there still remains some residual chirp on this IGM, because the dispersion was characterized by a measurement taken in a different measurement path with slightly different optical components.

6. Comparison between stabilization and post-correction

It is interesting to note the similarities between this setup and one which uses the CW lasers as a frequency reference to stabilize the frequency combs. In fact, the beating signals generated between the CW lasers and the combs are exactly the same. The differences arise in the way this information is used. When trying to stabilize the combs, one needs two actuators along with the associated electronics. Even then, one can only correct for the fluctuations that are within the actuator's bandwidth, and chances are that some information on faster fluctuations is available in the beating signal but cannot be used because of actuator bandwidth limitations.

With moderately stable CW oscillators, the ideal configuration would be to measure the beating to serve in post-correction while at the same time closing a low-speed servo loop based on the referencing information. Note that the combs are not locked onto the CW lasers, the CW lasers only serve as intermediate oscillators to compare the two combs, exactly like in the post-correction algorithm.

7. Conclusion

We have shown that the referencing technique for dual-comb interferometry could be significantly improved by using CW lasers as intermediate oscillators. This opens up the full resolution in spectroscopy measurements and the full distance range in optical coherence reflectometry/linear sampling applications. The concept was demonstrated with a spectroscopy measurement with 2 sec averaging time, where the full mutual coherence of the combs was recovered by the technique. Such a referencing technique lowers the requirements on the stabilization servo and for many applications, removes the need to operate a second servo loop on each laser to stabilize the f_{CEO}. One way to improve the current implementation would be to use reference lasers further apart in the optical band, to lower the effect of additive noise on the residual jitter. Future work includes implementing this referencing technique in real-time, to enable continuous measurement of a sample.

#134906 - $15.00 USD Received 9 Sep 2010; revised 15 Oct 2010; accepted 15 Oct 2010; published 20 Oct 2010

A. Mathematical derivation of the referencing signals

This section derives the expression for the beating of two pulse trains on a photodetector starting from the only assumption that the shape of each pulse stays the same over the time of the measurement. The result is valid even for pulse trains with fluctuating repetition rate and CEO, confirming the expectation that the cFTS signals can be described by only two parameters: the repetition rate difference and the CEO difference.

To derive the expression for the referencing signals, we start with a simple situation, where a single pair of pulses is filtered by a narrow-band optical filter. The two filtered pulses are then focused on a photodetector. We wish to obtain the expression describing the electrical signal at the output of the detector.

Each pulse comes from a source with a much larger bandwidth than the filter. Hence, we can approximate each pulse with a Dirac impulse. We use the complex notation to represent the electrical field from the laser, $s_1(t)$, at the input of the optical filter:

$$s_1(t) = \delta(t - T_{r1}) \exp(j\varphi_1), \tag{14}$$

where T_{r1} is the arrival time and φ_1 is the phase of the pulse. The impulse response of the filter is:

$$h_1(t) = a_1(t) \exp(j2\pi f_{c1} t), \tag{15}$$

where $a_1(t)$ is the baseband impulse response without the carrier frequency and f_{c1} is the central frequency of the filter. The output of the filter is the convolution of the input pulse and the impulse response:

$$s_{1f}(t) = s_1(t) * h_1(t) = a_1(t - T_{r1}) \exp\left[j2\pi f_{c1}(t - T_{r1}) + j\varphi_1\right]. \tag{16}$$

The response of the filter to the second pulse has the same form, but the arrival time is now T_{r2} and the phase is φ_2:

$$s_{2f}(t) = s_2(t) * h_1(t) = a_1(t - T_{r2}) \exp\left[j2\pi f_{c1}(t - T_{r2}) + j\varphi_2\right]. \tag{17}$$

For convenience, we define $\Delta T_r = T_{r2} - T_{r1}$ and $\Delta\varphi = \varphi_2 - \varphi_1$. The electrical signal at the output of the photodetector is proportional to:

$$s_d(t) = h_d(t) * \|s_{1f}(t) + s_{2f}(t)\|^2 \tag{18}$$

$$s_d(t) = h_d(t) * \left(\|s_{1f}\|^2(t) + \|s_{2f}(t)\|^2 + 2\Re\{s_{1f}(t)s_2^*(t)\}\right), \tag{19}$$

where $h_d(t)$ is the photodetector's impulse response. We consider only the product term between the two fields and use the complex signal instead of only the real part. The factor of 2 is also not included in order to the keep the expressions as simple as possible. The quantity of interest will be labeled $\tilde{s_d}(t)$:

$$\tilde{s_d}(t) \equiv h_d(t) * (s_1(t)s_2^*(t)) \tag{20}$$

$$\tilde{s_d}(t) = \int_{u=o}^{T_d} a_1(t - T_{r1} - u) a_1^*(t - T_{r2} - u) h_d(u) \exp\left[j2\pi f_{c1}\Delta T_r + j\Delta\varphi\right] du \tag{21}$$

$$\tilde{s_d}(t) = \int_{u=o}^{T_d} a_1(t - T_{r1} - u) a_1^*(t - T_{r2} - u) h_d(u) du \exp\left[j2\pi f_{c1}\Delta T_r + j\Delta\varphi\right]. \tag{22}$$

T_d is the time over which the detector's impulse response $h_d(t)$ is non-zero. To evaluate this integral, we first point out that the impulse response of the optical filter $h_1(t)$ is much shorter than the duration of the detector's impulse response. Hence, $h_d(t)$ is essentially constant over

#134906 - $15.00 USD Received 9 Sep 2010; revised 15 Oct 2010; accepted 15 Oct 2010; published 20 Oct 2010

the time where $a_1(t-T_{r1}-u)$ is non-zero, which is around $u=t-T_{r1}$. Also, the limits of integration can be changed to $[-\infty,\infty]$ without affecting the result since $a_1(t)$ has a smaller support than the actual limits $[0,\ T_{pd}]$. We can then write:

$$\tilde{s_d}(t) \approx h_d(t-T_{r1}) \int_{u=-\infty}^{\infty} a_1(t-T_{r1}-u)a_1^*(t-T_{r2}-u)du \exp\left[j2\pi f_{c1}\Delta T_r + j\Delta\varphi\right] \tag{23}$$

We can now see that the integral corresponds in fact to the autocorrelation of the baseband part of the impulse response of the filter:

$$A_1(\tau) \equiv \int_{u=-\infty}^{\infty} a_1(u)a_1^*(u+\tau)du, \tag{24}$$

so that

$$\tilde{s_d}(t) \approx h_d(t-T_{r1})A_1(\Delta T_r)\exp\left[j2\pi f_{c1}\Delta T_r + j\Delta\varphi\right] \tag{25}$$

This completes the derivation for the electrical signal produced by a single filtered pulse pair which is incident on a photodetector. When the signal is a pulse train, each pulse pair which overlaps temporally will produce a signal described by this expression, possibly with a different ΔT_r and $\Delta\varphi$. Since there will be no interaction from pulses that are temporally separated by more than the time of the filter's impulse response, we can simply write the electrical signal for the interference of the two pulse trains as the sum of the signal to each pulse pairs. We use the index k to indicate the k-th pulse pair. Each pulse pair will have a different ΔT_r and $\Delta\varphi$ and consequently we redefine them to be functions of k.

$$r_1(t) = \sum_k h_d(t-T_{r1}(k))A_1(\Delta T_r(k))\exp\left[j2\pi f_{c1}\Delta T_r(k) + j\Delta\varphi(k)\right] \tag{26}$$

This expression describes an electrical pulse train with a pulse at $T_{r1}(k)$, for each value of k. The amplitude of each pulse of this pulse train is modulated by the interference of the optical signals $A_1(\Delta T_r(k))\exp\left[j2\pi f_{c1}\Delta T_r(k) + j\Delta\varphi(k)\right]$. We now extract the amplitude of each electrical pulse by taking one sample per incident optical pulse pair, synchronized with the electrical pulse train $\sum_k h_d(t-T_{r1}(k))$. The discrete-time signal becomes:

$$r_{1d}[k] = h_d(0)A_1(\Delta T_r(k))\exp\left[j2\pi f_{c1}\Delta T_r(k) + j\Delta\varphi(k)\right] \tag{27}$$

To simplify further, we choose a gain on the sampler such that $h_d(0)=1$. Also, the same derivation could be done for a second optical filter with a central frequency f_{c2} instead of f_{c1}. This way, we obtain the following referencing signals:

$$r_{1d}[k] = A_1(\Delta T_r(k))\exp\left[j2\pi f_{c1}\Delta T_r(k) + j\Delta\varphi(k)\right] \tag{28}$$

$$r_{2d}[k] = A_2(\Delta T_r(k))\exp\left[j2\pi f_{c2}\Delta T_r(k) + j\Delta\varphi(k)\right] \tag{29}$$

If instead the pulse trains are filtered by an arbitrary sample, the electrical signal on the photodetector could be derived in a very similar way to obtain:

$$s_{md}[k] = A_m(\Delta T_r(k))\exp\left[j2\pi f_m\Delta T_r(k) + j\Delta\varphi(k)\right] \tag{30}$$

This time, $A_m(\tau)$ would be the autocorrelation of the baseband part of the sample's impulse response, filtered by the crosscorrelation of the baseband electrical field of the pulses used for probing. If only one comb probes the sample, $A_m(\tau)$ will be the sample's baseband impulse response, filtered by the probing pulse's shape and the time-reversed shape of the other pulse shape.

#134906 - $15.00 USD Received 9 Sep 2010; revised 15 Oct 2010; accepted 15 Oct 2010; published 20 Oct 2010

Acknowledgements

The authors would like to thank the Natural Sciences and Engineering Research Council of Canada, the Canadian institute for photonic innovations and Telops Inc. for their financial support.

#134906 - $15.00 USD Received 9 Sep 2010; revised 15 Oct 2010; accepted 15 Oct 2010; published 20 Oct 2010